Sulfur Dioxide Oxidation in Slurries of Activated Carbon

HIROSHI KOMIYAMA and J. M. SMITH

Department of Chemical Engineering
University of California
Davis, California 95616

Part I. Kinetics

Dynamic adsorption and reaction studies were made for the catalytic oxidation of sulfur dioxide in aqueous slurries of activated carbon at room temperature and atmospheric pressure. For the small particles (d_p = 0.03 mm) of carbon used, mass transfer resistances were of minor importance so that the data could be analyzed in terms of the kinetics of the chemical reaction. Quantitative evaluation of mass transfer effects, including intraparticle diffusion, is presented in Part II.

The rate was first order in oxygen concentration in the liquid and zero order with respect to SO_2. The rate decreased with increasing H_2SO_4 concentration in the liquid. This was explained by the decrease in solubility of oxygen in the solution rather than by a change in reaction rate constant. The adsorption and rate data together suggest that the controlling step in the mechanism is the adsorption of oxygen on active sites of the carbon surface. The low concentration of oxygen in water (due to its low solubility) reduces its rate of adsorption.

SCOPE

Activated carbon is known to catalyze oxidation of SO_2 at room temperature. This provides a potential process for continuous removal of sulfur dioxide from gas streams. The comprehensive review of Hartman et al. (1971) notes that chemisorbed oxygen has a role in the oxidation process and that the presence of water removes the adsorbed SO_3 molecules, thus renewing the active sites. Also these authors found that H_2SO_4 slows the rate of oxidation. Unless water is continuously added the buildup of H_2SO_4 in the solution (containing the activated carbon) will ultimately cause the reaction to stop.

The kinetics of the reaction, with water present, are not well understood, particularly the role of oxygen and H_2SO_4. Hartman and Coughlin (1972) interpreted trickle-bed reactor data in terms of kinetics which supposed that the surface rate between adsorbed atomic oxygen and adsorbed sulfur dioxide to be rate determining. Since the inlet concentration to the reactor was constant, the results were not a stringent test of the kinetics model. Also intraparticle diffusion was not separated from the intrinsic rate constant. These authors also pointed out the effect of H_2SO_4 in decreasing the solubility of sulfur dioxide in aqueous solutions. Other studies of this system have not analyzed the kinetics of the oxidation reaction. Joyce et al. (1970) reported trickle-bed studies of the recovery of SO_2 from gas streams. Sulfuric acid of 12% concentration was obtained with an excess of oxygen and at 100°C. Seaburn and Engel (1973) compared several activated carbons of different particle sizes in terms of capacity for adsorbing SO_2 and catalytic activity for the oxidation reaction. Intraparticle diffusion resistances for the various carbons were not considered.

The present work was undertaken to clarify the adsorption and reaction characteristics of the oxygen-sulfur dioxide-activated carbon-water system in a three-phase slurry reactor. Part I presents an analysis of data showing predominantly the chemical kinetics of the oxidation. Of specific interest was the rate controlling step and the effect of H_2SO_4. Then in Part II, with particles of different sizes, the quantitative significance of the several mass transfer effects is presented.

CONCLUSIONS AND SIGNIFICANCE

Dynamic experiments where SO_2, O_2, and He were fed to the slurry indicated a pseudo steady state of several hours duration during which the rate was constant. The results showed that this rate, which was retarded up to 20% by fluid-to-particle resistance and intraparticle mass transfer resistance in the liquid-filled pores, was first order in dissolved oxygen and zero order in sulfur dioxide. Adsorption of SO_2 was found to be very rapid, and the equilibrium isotherm was strongly nonlinear, following a Freundlich equation. Experiments pretreating the catalyst with oxygen showed that adsorbed O_2 affected the rate. Approximate calculations showed that the rate of oxygen adsorption to be of the same order as the rate of reaction. These results and the first-order dependency was interpreted to mean that the controlling step in the oxidation was the adsorption of oxygen. The decrease in rate

H. Komiyama is on leave from University of Tokyo.

observed for increasing H_2SO_4 concentrations in the slurry liquid compares reasonably well with the corresponding decrease in solubility of oxygen. The change in solubility rather than a decrease in intrinsic rate is believed to be responsible for the effect of H_2SO_4. The small effect of liquid concentration on the adsorption isotherm for H_2SO_4, and the relatively low surface converge of H_2SO_4 provide additional evidence for this conclusion.

Pittsburgh Activated Carbon (PAC), type BPL, whose properties are given in Table 1 is known to adsorb SO_2 and to catalyze its oxidation to SO_3 (Joyce et al., 1970; Seaburn and Engel, 1973). This material, crushed and sieved to particles less than 250 mesh size (average d_p = 0.03 mm) in order to reduce intraparticle diffusion resistance, was employed for adsorption and reaction studies. Larger particles of the same material were used in Part II to evaluate mass transfer effects. Adsorption isotherms were measured for SO_2 and H_2SO_4, at 22° to 25°C and atmospheric pressure, in slurries of the particles in water or aqueous H_2SO_4 solutions. Subsequently, oxidation rates were measured at the same temperature as a function of O_2, SO_2, and H_2SO_4 concentrations and preadsorption of oxygen on the carbon. The adsorption capacity of PAC for oxygen was too small to measure by the same method.

APPARATUS AND PROCEDURE

The essential feature of the apparatus, shown in Figure 1, was a 10-cm high, 10-cm diameter, cylindrical Pyrex adsorber, or reaction vessel, equipped with an impeller as described elsewhere (Furusawa and Smith, 1973). The slurry was prepared first and then gas streams were mixed to the desired composition and introduced continuously through a fritted-glass disk, 12 mm in diameter and 21 mm in height, located near the bottom of the Pyrex vessel. The carbon particles were pretreated with helium at 250°C to remove adsorbed oxygen before preparing the slurry.

In preparation for a run, helium was passed through the adsorber for 30 min. Then, the three-way valve was turned to discharge the gas stream to the vent while the regulators were adjusted to give the desired composition of SO_2, O_2, and He. The run was initiated by using the 3-way valve to introduce a step function of the gas mixture to the vessel. After removal of most of the water vapor in an ice trap, a seven-way sample valve was used to introduce periodically a sample to a gas chromatograph for determination of SO_2 or O_2.

TABLE 1. SCOPE OF MEASUREMENTS

A. Properties of Pittsburgh Activated Carbon
   surface area, m^2/g = 800
   porosity of particles, ϵ_p = 0.64
   particle density, ρ_p, g/cm^3 = 0.80
   particle diameter d_p (arithmetic mean), = 0.03 mm

B. Volume of liquid in adsorber, V_L, cm^3
   = 900 (Pyrex adsorber)
   = 500 (measuring cylinder)

C. Mass of solid, M_s, g = 20 to 30 (adsorption runs)
   = 1 to 5 (reaction runs)

D. Concentrations
   Inlet gas stream, %:
   SO_2 = 2.3, 4.0 or 7.7 (adsorption runs)
   0.3 to 9.0 (reaction runs)
   O_2 = 5.2 to 21
   H_2SO_4 in liquid, g. equiv./liter = 0 to 10.8

E. Total gas flow rate, F, cm^3/min.
   = 2000 (Pyrex adsorber)
   1000 (measuring cylinder)

F. Impeller speed, rev./min. = 550 ~ 650

A Porapack-S column (1 ft. long) at 60°C gave a good separation of SO_2 and O_2 with an analysis time of about 3 min. To reduce uncertainties in the rate data, the volumes of tubing between sample injection and sample valve were minimized. The volume between the top of the slurry in the vessel and the sample valve was about 800 cm^3. Since the total flow rate was 2000 cm^3/min., the residence time in this volume was 0.4 min. A correction for this time was made although it is relatively short with respect to the period required for significant changes in concentration in the effluent stream (for example, Figure 2).

ADSORPTION OF SULFUR DIOXIDE

Dynamic absorption and adsorption measurements were made for sulfur dioxide in water and in aqueous slurries of PAC. Figure 2 shows the experimental data points for an inlet gas containing 2.3 vol. % SO_2 (in helium). Similar data were obtained for feed gases containing 4.0 and 7.7 SO_2.

To establish equilibrium isotherms from these data, it is necessary to know the extent of mixing in the gas (bubbles) and liquid phases. In a well-agitated slurry with gas bubbles, Siemes and Weiss (1957) found mixing in the liquid to be rapid. Hence, complete mixing was assumed for this phase. Even for an agitated slurry the bubble stream is not well mixed (Juvekar and Sharma, 1973; Misic and Smith, 1971). The latter authors showed that plug flow of gas well represented their data for benzene adsorption in an agitated, aqueous slurry of activated carbon. They derived the following expression

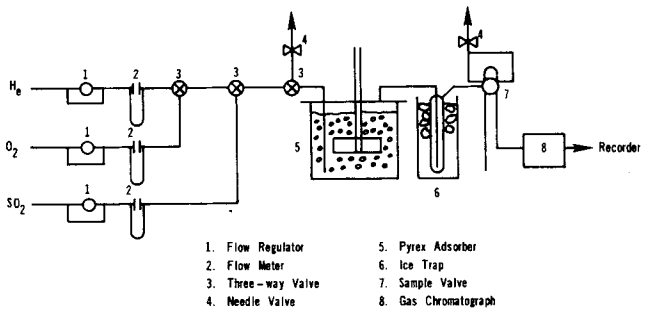

Fig. 1. Schematic diagram of apparatus.

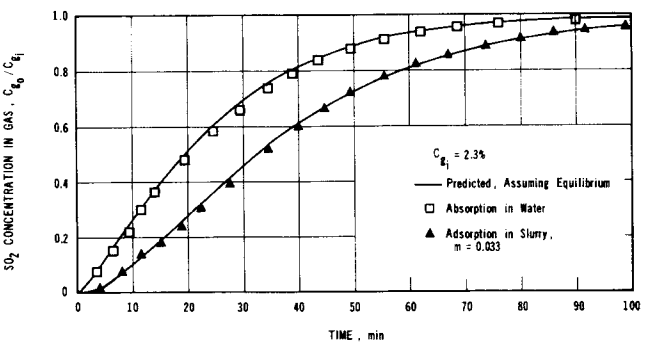

Fig. 2. Dynamic adsorption of SO_2.

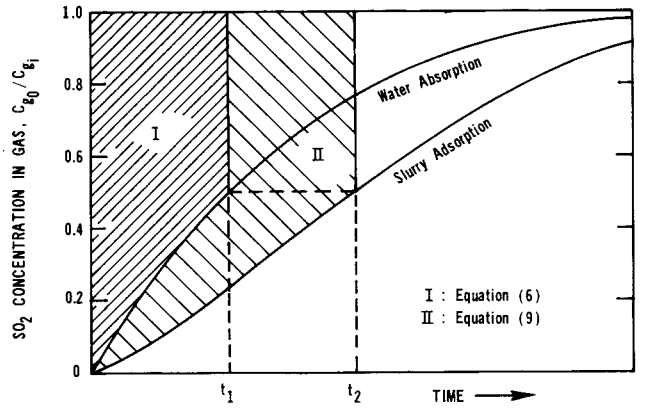

Fig. 3. Graphical integration method for isotherms.

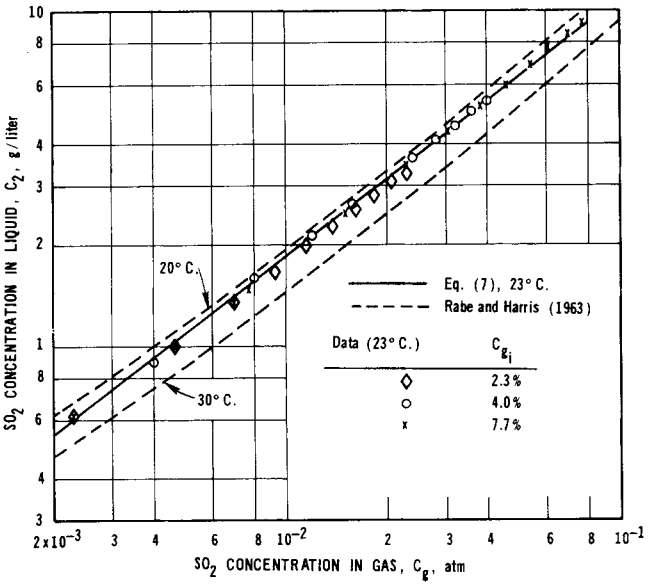

Fig. 4. Gas-liquid equilibrium for SO_2 and water.

for the axial concentration profile $C_g(z)$ in the gas phase:

$$C_g(z) = H\,C_L + (C_{go} - H\,C_L)\exp(-\alpha z) \qquad (1)$$

$$\alpha = \frac{k_L\,a_b\,V_b}{HFL} \qquad (2)$$

Although Henry's law is not obeyed for SO_2 absorption in water, a linearized estimate of H can be used in Equation (2) to approximate α. This α is about 20 cm^{-1} versus 0.5 for benzene (Misic and Smith's system) because of the larger solubility of SO_2 in water and because V_b was much larger in the present apparatus. For an α value of 20 and all values of z greater than a fraction of a centimeter, Equation (1) reduces to the equilibrium relation:

$$C_g(z) = H\,C_L \qquad (3)$$

This analysis shows that equilibrium exists between SO_2 in the gas and liquid, except where the bubble enters the liquid. Therefore, since C_L is constant through the vessel, C_g also will be constant, regardless of the extent of mixing in the gas flow.

The time constant for liquid-to-solid diffusion is about $1/k_s a_s$, which is about 0.01 s using the value of k_s determined in Part II. Intraparticle diffusion plus adsorption time is about $K\,R^2/D_e$. From Part II the linearized adsorption equilibrium constant K is about 30 and $D_e = 6.8 \times 10^{-6}$ cm^2/s. Hence this time constant is about 40 s. Both of these mass transfer times are much smaller than the time for the overall adsorption process. For example, the half-time from Figure 2 is about 30 min. It was concluded that mass transfer effects were insignificant for the adsorption measurements. Then mass conservation equations for SO_2 absorption into water alone, and for absorption and adsorption into the slurry, may be written

$$V_L\frac{dC_L}{dt} = F(C_{gi} - C_{go}) \qquad (4)$$

$$M_s\frac{dq}{dt} + V_L\frac{dC_L}{dt} = F(C_{gi} - C_{go}) \qquad (5)$$

Equation (4) can be integrated, using the data in the upper curve of Figure 2, to give C_L as a function of time:

$$C_L(t) = \frac{F}{V_L}\int_0^t [C_{gi} - C_{go}(t)]dt \qquad (6)$$

The resultant curve for C_L vs. t is shown schematically in Figure 3. In this figure the shaded area, marked I, is proportional to the integral in Equation (6) from 0 to t_1.

Each measured value of C_{go} obtained during an absorption run can be used with Equation (6) to obtain the corresponding C_L. Since it has been shown that the exit gas stream is in equilibrium with the liquid, these sets of C_{go} and C_L locate points on the absorption isotherm. The results are shown in Figure 4 for the three absorption runs corresponding to the three C_{gi} values. Also shown in the figure are the data of Rabe and Harris (1963) at 20° and 30°C. Our data at 23°C can be expressed by a Freudlich-type equation

$$C_L = 2.24\,C_g^{0.768} \qquad (7)$$

The adsorption isotherm for SO_2 between water and PAC can be obtained from the data in Figure 2 by a modification of the same procedure. Integration of Equation (5) gives

$$M_s\,q + V_L\,C_L = \int_0^t F[C_{gi} - C_{go}(t)]dt \qquad (8)$$

The integral can be evaluated by using the data given in the lower curve of Figure 2. To obtain q corresponding to a given C_L, the integration should be carried out to a time corresponding to the same SO_2 concentration in the gas. The procedure is illustrated in Figure 3. Suppose it

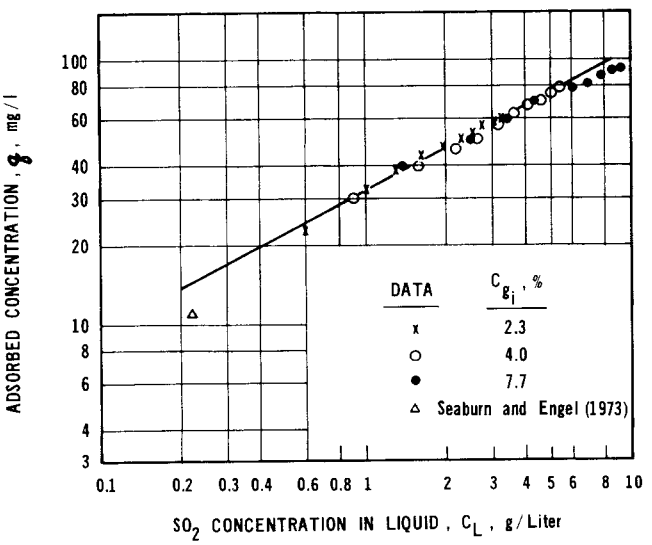

Fig. 5. Adsorption isotherm for sulfur dioxide on PAC at 23°C.

is desired to obtain q in equilibrium with C_L corresponding to $C_{go} = 0.5\ C_{gi}$. Figure 3 shows that this C_L is given by evaluating the integral in Equation (6) from 0 to t_1. Then the integral in Equation (8) would be evaluated from 0 to t_2. Since C_L is known, q can be calculated from Equation (8). Alternately, Equation (6) and (8) can be combined to give q directly from the data in Figure 2:

$$q = \frac{F}{M_s}\left\{ \underbrace{\int_0^{t_2} [C_{gi} - C_{go}(t)]dt}_{\text{slurry}} - \underbrace{\int_0^{t_1} [C_{gi} - C_{go}(t)]dt}_{\text{water alone}} \right\} \quad (9)$$

The area in Figure 3 marked II is proportional to the difference between the two integrals. The results for q vs. C_L are shown in Figure 5 for the three adsorption runs. The agreement in the intermediate region of the figure between the data for the run with the highest C_{gi}(7.7% SO_2) and those for C_{gi} of 4.0% and 2.3% indicates that equilibrium is achieved between solid and liquid phases at any time during the adsorption runs. The Freudlich representation of the isotherm is

$$q_{SO_2} = 0.180\ C_L^{0.532} \quad (10)$$

As a check of the calculations, Equations (4) and (5) were solved numerically to predict C_{go}/C_{gi} vs. time, using Equations (7) and (10) for the relations between C_L and C_g and q and C_L. The solid-line curves in Figure 2 resulted from these calculations.

Seaburn and Engel (1973) contacted a slurry of PAC in water with a stream of 560 ppm of SO_2 in nitrogen at room temperature until the SO_2 in the exit stream exceeded 90% of the inlet concentration. Assuming equilibrium, the point corresponding to these conditions is also shown in Figure 5.

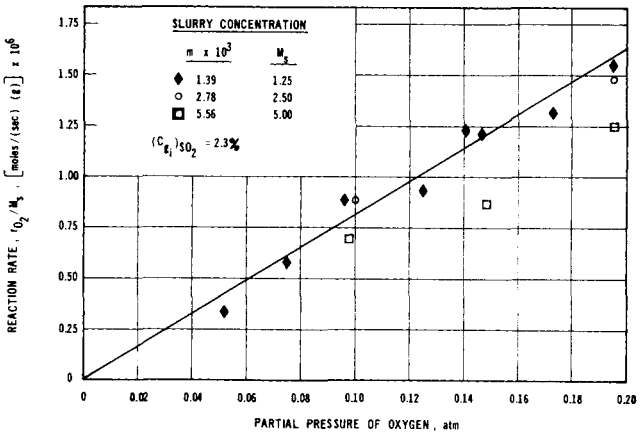

Fig. 8. Reaction rate vs. partial pressure of oxygen.

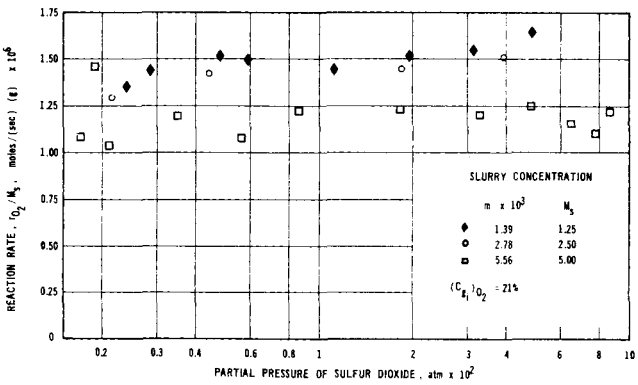

Fig. 9. Reaction rate vs. partial pressure of sulfur dioxide.

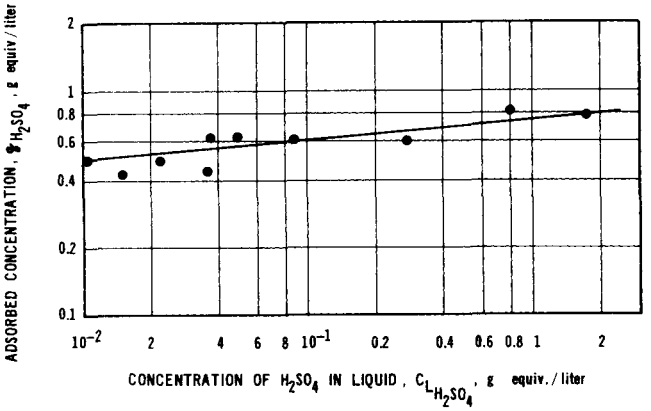

Fig 6. Adsorption isotherm for sulfuric acid on PAC at 22°C

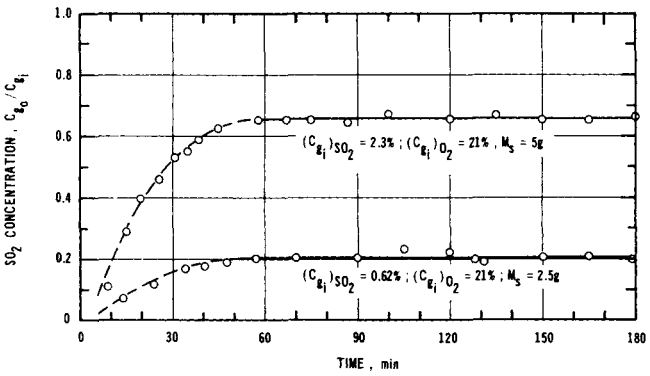

Fig. 7. Typical concentration vs. time curve for reaction experiment (25°C).

ADSORPTION OF H_2SO_4

The isotherm at 23°C was determined by adding a known amount of H_2SO_4 solution to a flask containing the agitated slurry of PAC and by analyzing the solution for H_2SO_4 after equilibrium was reached. Strongly nonlinear results were obtained as shown by the rather flat line in Figure 6. The Freundlich equation corresponding to the line in the Figure is

$$q_{H_2SO_4} = 1.39 \times 10^{-4}\ C_{L,H_2SO_4}^{0.091} \quad (11)$$

OXIDATION REACTION

The reaction experiments were carried out in the same way as the SO_2 adsorption runs, except that oxygen was added to the inlet gas stream. Figure 7 shows the SO_2 concentration in the effluent gas for typical runs. The long period (several hours) of constant exit gas concentration occurred for each run. This permitted calculation of the rate of oxidation, in moles/s for the whole slurry, from the equation

$$r_{O_2} = \frac{1}{2} r_{SO_2} = \frac{1}{2} F\ (C_{gi} - C_{go})_{SO_2} \quad (12)$$

where C_{go} is the constant concentration in the effluent gas. During this constant-rate period the H_2SO_4 concentration

in the liquid was very low, approaching zero. Hence, H_2SO_4 did not retard the rate significantly for these data, in contrast to the results shown later when the slurry liquid was an aqueous solution of H_2SO_4. It would be expected that the curves in Figure 7 would ultimately rise, reflecting the reduced rate of reaction when the H_2SO_4 concentration in the liquid became large. The increase in SO_2 in the exit gas at low time values is due to the finite rate of build up of SO_2 concentrations in the water and on the carbon particles.

The rates calculated from Equation (12) are shown plotted as r_{O_2}/M_s versus partial pressures of oxygen and of sulfur dioxide in Figures 8 and 9 for three concentrations of carbon particles in the slurry. Since these rates per unit mass are essentially the same for the two lowest slurry concentrations, bubble-to-liquid mass transfer resistance is insignificant at these low concentrations. However, retardation of the rate due to fluid-to-particle and intraparticle mass transfer is included in the r_{O_2} values. The results in Part II indicate for the small particles used (average $d_p = 0.03$ mm) that the rate is reduced by no more than 20% due to these two transport processes and that the gas phase resistance is negligible. As the objective here is to establish the reaction order and the rate-determining step rather than quantitative values of the rate constant, such r_{O_2} will be assumed to represent intrinsic kinetics at the reaction sites on the pore surface.

The lines in Figures 8 and 9 suggest that the rate is first order in oxygen and zero order in sulfur dioxide so that r_{O_2} is given by the expression

$$r_{O_2} = k_r' \left(\frac{M_s}{\rho_p}\right) C_{L,O_2} \qquad (13)$$

where k_r' is the rate constant based upon unit volume of particles and includes the effect of the small fluid-to-particle and intraparticle resistances associated with the small ($d_p = 0.03$ mm) particles. Also the k_r' value corresponding to the data in Figures 8 and 9 are for a very low H_2SO_4 concentration in the liquid.

Effect of H_2SO_4

Additional kinetic runs were made in the same way when the slurry liquid consisted of aqueous solutions of H_2SO_4 up to 11 normal. Because of corrosion, the data were obtained in a 500 cm³ glass graduate using the same fritted disk for introducing the gas, but with a magnetic stirrer (teflon-coated, iron cylinder 6 mm in diameter and 22 mm long). This arrangement gave less agitation so that bubble-to-liquid mass transfer affected the rate, even at low concentrations of PAC particles in the slurry. This effect on the rate was eliminated by analyzing data taken for various slurry concentrations. For a first-order reaction the rate may be expressed in terms of the reaction and in terms of the bubble-to-liquid mass transfer coefficient k_L:

$$r_{O_2} = k_L\, a_b\, V_b\, (C^*_{O_2} - C_{L,O_2}) = k_r' \left(\frac{M_s}{\rho_p}\right) C_{L,O_2} \qquad (14)$$

where $C^*_{O_2}$ is given by $C_{g_{O_2}}/H$ since there is negligible resistance to mass transfer in the gas phase for slightly soluble oxygen. Eliminating the bulk liquid concentration C_{L,O_2} from these equations leads to

$$\frac{1}{r_{O_2}} = \frac{1}{k_L\, a_b\, V_b\, C^*_{O_2}} + \frac{\rho_p}{k_r'\, M_s\, C^*_{O_2}} \qquad (15)$$

The values of r_{O_2} obtained for various H_2SO_4 concentrations in the slurry are shown in Figure 10, plotted as $1/r_{O_2}$ vs. $1/M_s$. The partial pressure of SO_2 in the liquid

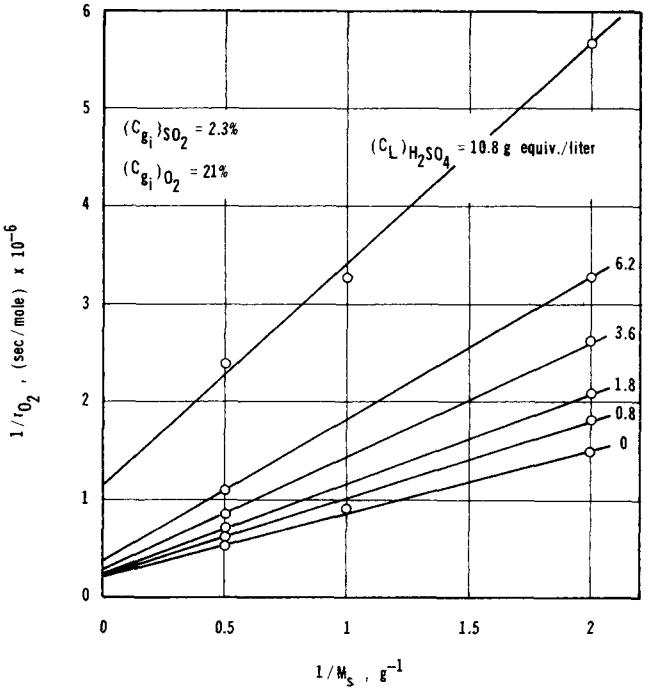

Fig. 10. Effect of sulfuric acid on the rate (25°C).

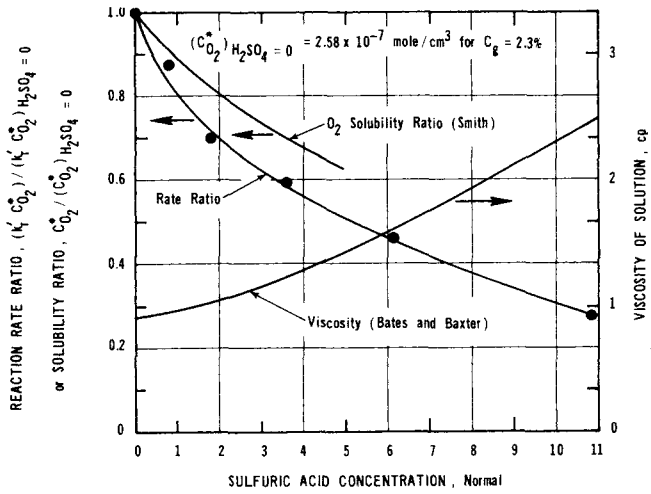

Fig. 11. Dependency of reaction rate and oxygen solubility on sulfuric acid concentration (25°C).

changes with M_s, but this does not affect the rate because of the zero-order effect shown in Figure 9. For the large excess of oxygen used in these experiments, the oxygen concentration is nearly constant. Then according to Equation (15) the lines in Figure 10 should be linear and the rate $k_r'\, C^*_{O_2}$ can be determined from their slopes. The results so obtained are shown in Figure 11, plotted as the ratio of the rate at a finite H_2SO_4 concentration to that at zero concentration. The rate decreases continually as $C_{H_2SO_4}$ increases, reaching about ¼ of its original value for 11 normal H_2SO_4. The slope of the line for zero concentration of H_2SO_4 in Figure 10 corresponds closely to the data for r_{O_2} shown in Figure 9.

Mechanism and Rate-Controlling Step

The zero-order effect shown in Figure 9 suggests that SO_2 does not participate in the rate-controlling step of the reaction. Sulfur dioxide is strongly adsorbed (Figure 5), but the adsorption rate appears to be extremely rapid with respect to the rate of oxidation. Evidence for this

is that equilibrium adsorption could be assumed in analyzing the dynamic adsorption data, while Figure 7 shows that the rate of oxidation is finite.

The first-order effect of oxygen (Figure 8) indicates that the controlling step is either: (1) the adsorption of oxygen, (2) reaction between adsorbed molecular oxygen and sulfur dioxide on the catalyst surface, or (3) reaction between dissolved O_2 in the liquid and adsorbed SO_2. Results for pretreatment of the catalyst with oxygen (Figure 12) demonstrate that adsorbed oxygen greatly affects the rate, thus excluding the third possibility. Reaction between molecularly adsorbed oxygen and sulfur dioxide to produce SO_3 is not consistent with the observed zero-order effect of SO_2. Reaction between adsorbed atomic oxygen and SO_2 is more plausible, but for this step to be controlling the rate would be half-order in oxygen. It was concluded that the reaction occurs by adsorption of oxygen atoms followed by surface reaction and that the controlling step is the adsorption process:

$$O_2(aq.) + 2X \rightarrow 2O \cdot X \qquad (16)$$

The retardation of the rate by H_2SO_4 in the liquid is believed to be caused primarily by the reduced solubility of O_2 in sulfuric acid solutions. Such solubility data at 25°C are available (Smith, 1929) up to concentrations of 5 normal. These data, plotted as the ratio of the solubility to that in pure water, are also indicated in Figure 11 and show the same trend as the rate results. Some deviation between the two curves is expected because the viscosity of the aqueous solution increases as the concentration of H_2SO_4 increases. These data (Bates and Baxter, 1929) are shown by the lower curve in Figure 11. The increase in viscosity would reduce the diffusivity of oxygen in the liquid, and hence, increase both the fluid-to-particle and intraparticle mass transfer resistances above the 20% corresponding to zero concentration of H_2SO_4. The effects of these increased resistances would become more important as $C_{H_2SO_4}$ increases and lower the rate-ratio curve in Figure 11. Interpreted in this way, the intrinsic rate constant k_r is believed to be nearly independent of H_2SO_4. The rate decrease is unlikely to be due to blocking of catalyst sites by H_2SO_4 because the adsorption isotherm is nearly flat (Figure 6). The fractional surface coverage by H_2SO_4 for a 2 normal liquid concentration is estimated to be 0.11.

As a test of the importance of adsorption of oxygen on the rate, dynamic reaction experiments were made, in the usual way, after pretreating the slurry with oxygen. The slurry liquid was 0.05 normal H_2SO_4 to avoid a significant effect of H_2SO_4 production on the rate. The procedure was to pretreat the fresh slurry with a stream of pure oxygen for various times and then change the feed gas to the reaction stream of 2.3% SO_2, 21% oxygen, and 76.7% helium. Then the SO_2 concentration was periodically measured for the first few minutes after the reaction-gas flow was started. The results, seen in Figure 12, show that the exit SO_2 concentration was lower after pretreatment with oxygen. This was interpreted to mean that preadsorbed oxygen increased the reaction rate. The data show also that the longer the pretreatment period the greater the increase in rate. The shaded area in Figure 12 corresponds to the additional amount of O_2 reacted due to the 30-s pretreatment with pure oxygen. Some oxygen is desorbed during the reaction period of about 8 min. If this is neglected, the shaded area is proportional to the net amount of oxygen adsorbed during the pretreatment, and this amount is 1.0×10^{-4} g mole. Then an approximate value for the average rate r_{Ad} is 3.3×10^{-6} g mole/s. From this rate the adsorption rate con-

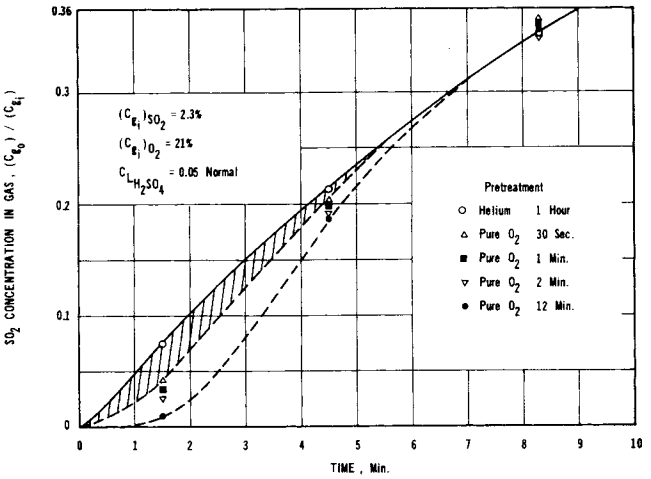

Fig. 12. Effect of oxygen pretreatment on reaction.

stant, corresponding to the equation

$$r_{Ad} = k'_{Ad} C_{L,O_2} \left(\frac{M_s}{\rho_p} \right) \qquad (17)$$

is $k'_{Ad} = 1.8\ s^{-1}$. This is the same order of magnitude (it is about one third) as the value of k_r' obtained from Equation (13) using the reaction data of Figure 8. The data in Figure 12 and the agreement between the two rate constants are considered to be further evidence that the adsorption of oxygen controls the rate of oxidation. Actually, the net amount adsorbed during pretreatment will be greater than 1×10^{-4} g mole if oxygen is desorbed during the reaction period. To provide information about desorption, pretreatment experiments were made with helium. After an initial treatment with oxygen for 20 min., pure helium was passed through the slurry for different times before the reaction-gas flow was started. These data showed that adsorbed oxygen was desorbed within a few minutes. Assuming that desorption occurs under reaction conditions as well as when only helium is present, these experiments indicate that the calculated rate constant k'_{Ad} is less than the expected value. That is, the shaded area in Figure 12 measures the adsorbed oxygen that reacts. This is less than the oxygen adsorbed, because of desorption.

Siedlewski (1965) reported that chemisorbed oxygen reacts with sulfur dioxide on activated carbon. He also found that the number of molecules of SO_3 produced was proportional to the number of active sites chemisorbing oxygen. Happel et al. (1973) suggested also that the adsorption of oxygen was the slowest step in the oxidation of SO_2 with a V_2O_5 catalyst. In contrast, Otake et al. (1971) found that the rate in the absence of water was controlled by the reaction between adsorbed species on the carbon surface. Differences in solubilities between SO_2 and O_2 in water could explain the discrepancy between Otake's results and those reported here. For example, for a gas phase containing 10% O_2 and 1% SO_2, the ratio of the equilibrium concentrations of O_2 to SO_2 in water is 0.005. Hence, the rate of adsorption of O_2 from the liquid could be the controlling step in a slurry reaction while the surface reaction step is rate-controlling in the gas-solid reaction.

It should be noted that for the relatively high concentrations of sulfur dioxide used in our work the carbon surface is essentially saturated with SO_2. Hence, a zero-order effect is expected. At lower and lower concentrations a condition would be reached where the sulfur dioxide concentration would influence the rate of oxidation.

ACKNOWLEDGMENT

Acknowledgment is made to the Donors of the Petroleum Research Fund administered by the American Chemical Society, for the partial support of this research. Also thanks are due to Pittsburgh Activated Carbon Division of the Calgon Corporation for supplying the carbon particles.

NOTATION

a_b = surface area of bubbles per unit volume of bubbles, cm^{-1}

a_s = outer surface area of particles per unit volume of particles, cm^{-1}

C_g = concentration in gas; C_{gi} and C_{go} refer to inlet and outlet streams, respectively; $mole/cm^3$

C_L = concentration in liquid; C^* is concentration in equilibrium with C_g; $mole/cm^3$ (For sulfuric acid g-equiv./cm^3)

d_p = particle diameter (assumed to be spherical), cm

F = total volumetric flow rate of gas, cm^3/s

H = ratio of equilibrium concentration in gas phase to that in liquid phase ($H = C_g/C^*$)

K = adsorption constant for linear isotherm ($\rho_p q = K C_L$)

k'_{Ad} = adsorption rate constant for oxygen, defined by Equation (17), s^{-1}

k_L = mass transfer coefficient from gas bubble interface to bulk liquid, cm/s

k_r' = apparent reaction rate constant defined by Equation (13); includes effects of mass transport resistances, s^{-1}

k_r = intrinsic rate constant at catalyst site, s^{-1}

k_s = mass transfer coefficient from liquid to particle, cm/s

L = total height of slurry above entrance of gas bubbles, cm

M_s = mass of liquid-free particles in slurry, g

m = fraction solids in slurry, $M_s/V_L\rho_L$

q = adsorbed concentration, mole/(g of carbon particles)

r_{Ad} = total adsorption rate of oxygen, mole/s

r_{O_2} = total reaction rate of oxygen; r_{SO_2} is rate for sulfur dioxide, mole/s

t = time, s

V_b = total volume of bubbles in slurry, cm^3

V_L = total volume of particle- and bubble-free liquid in slurry, cm^3

z = vertical distance measured from entrance of gas bubbles into slurry, cm

Greek Letters

α = parameter defined by Equation (2), cm^{-1}

ρ_L = density of particle-free and bubble-free liquid in slurry, g/cm^3

ρ_p = density of liquid-free particles, g/cm^3

ϵ_p = porosity of particles

LITERATURE CITED

Bates, S. J., and W. P. Baxter, *International Critical Tables*, **5**, 12 (1929).

Furusawa, T., and J. M. Smith, "Fluid-Particle and Intra-Particle Mass Transport Rates in Slurries," *Ind. Eng. Chem. Fundamentals*, **12**, 197 (1973).

Happel, J., M. A. Hnatow, and A. Rodriguez, "Use of Tracers in Study of Catalytic Oxidation of Sulfur Dioxide," *AIChE J.*, **19**, 1075 (1973).

Hartman, M., J. R. Polek, and R. W. Coughlin, "Removal of Sulfur Dioxide from Flue Gas by Sorption and Catalytic Reaction on Carbon," *Chem. Eng. Progr. Symp. Ser. No. 115*, **67**, 7 (1971).

Hartman, M., and R. W. Coughlin, "Oxidation of SO_2 in a Trickle-bed Reactor with Carbon," *Chem. Eng. Sci.*, **27**, 867 (1972).

Joyce, R. S., R. T. Lynch, R. F. Sutt, and G. S. Tobias, "Effective Recovery of Dilute SO_2," Third Joint Meeting of the Am. Inst. Chem. Engrs. and Inst. Mex. de Ing. Quimicos, (Denver) (1970).

Juvekar, V. A., and M. M. Sharma, "Adsorption of CO_2 in a Suspension of Lime," *Chem. Eng. Sci.*, **28**, 825 (1973).

Misic, D. M., and J. M. Smith, "Adsorption of Benzene in Carbon Slurries", *Ind. Eng. Chem. Fundamentals*, **10**, 380 (1971).

Otake, T., S. Tone, Y. Yokota, and K. Yoshirmura, "Kinetics of Sulfur Dioxide Oxidation over Activated Carbon," *J. Chem. Eng. Japan*, **4**, 155 (1971).

Rabe, A. E., and J. F. Harris, "Vapor Liquid Equilibrium Data for the Binary System, Sulfur Dioxide and Water," *J. Chem. Eng. Data*, **8**, 333 (1963).

Seaburn, J. T., and A. J. Engel, "Sorption of Sulfur Dioxide by Suspension of Activated Carbon in Water," *AIChE Symp. Ser. No. 134*, **69**, 71 (1973).

Siedlewski, Y. U., "The Mechanism of Catalytic Oxidation on Activated Carbon, The Role of Free Carbon Radicals in the Oxidation of SO_2 to SO_3," *Intern. Chem. Eng.*, **5**, 608 (1965).

Siemes, W., and W. Weiss, "Mixing of Liquids by Means of Gas Bubbles in Narrow Columns," *Chem. Ing. Tech.*, **29**, 727 (1957).

Smith, D. F., *International Critical Tables*, **3**, 271 (1929).

Part II. Mass Transfer Studies

Bubble-to-liquid, liquid-to-particle, and intraparticle mass transport effects were all found to be significant for some conditions in a three-phase slurry reactor operated for the oxidation of SO_2 at 25°C and 1 atm. In particular, intraparticle diffusion was important for particles as small as 99 microns (effectiveness factor = 0.45).

Effective diffusivities determined from reaction, desorption, and adsorption data for O_2, H_2SO_4, and SO_2 indicated that surface diffusion was appreciable for SO_2 but not for oxygen. These results are consistent with the kinetic results in Part I which suggested that the rate-controlling step was a chemisorption process for oxygen on the pore surface of the carbon particles.